

# High Resolution AVO

Jon Downton\*

Core Lab Reservoir Technologies Division, Calgary, AB  
University of Calgary, 301, 400-3rd Ave. S.W., Calgary, AB, T2P 4H2  
jdownton@corelab.ca

Laurence Lines

University of Calgary, Calgary, AB

## ABSTRACT

### Summary

This paper demonstrates a methodology to produce high-resolution AVO reflectivity attribute estimates similar to sparse spike deconvolution. The AVO estimate is performed prior to NMO avoiding the distortions and loss of frequency associated with this process. Long tailed a priori distributions are used to constrain the problem. The resulting sparse reflectivity is able to resolve thin layers and is more reliable than the estimates provided by the traditional AVO analysis that is performed on a sample-by-sample basis on NMO corrected gathers. This greater reliability is due to the classic trade-off between resolution and reliability. With the new method a few sparse reflectivity values are estimated with greater certainty than the dense reflectivity at every time sample as in the traditional AVO analysis.

### Introduction

We present a method for producing high-resolution estimates of AVO reflectivity attributes. The objective is to produce a sparse spike reflectivity series as output similar to that done by poststack sparse deconvolution (Levy and Fullagar, 1991; Sacchi, 1999; and Trad, 2002). Further, the methodology presented is analogous to the high-resolution Radon transform presented by Sacchi and Ulrych (1995). The new approach provides superior resolution and greater reliability than the traditional approach of first applying NMO and then performing AVO analysis.

The theory for this new algorithm is developed using a Bayesian formalism. Instead of the typical assumption of Gaussian probability distributions, various long-tailed distributions are used for the prior distribution. The likelihood model is based on the AVO NMO formalism (Downton and Lines, 2002) where the AVO and NMO inversions are performed simultaneously assuming some input wavelet. The inversion is nonlinear and must be solved using a bootstrap procedure. A synthetic seismic example is shown demonstrating the new methodology

## Theory

### *Convolutional model*

The convolutional model is used as the basis for the likelihood model. This model assumes the earth is composed of a series of flat, homogenous, isotropic layers. Ray tracing is done to map the relationship between the angle of incidence and offset. Transmission losses, converted waves, and multiples are not incorporated in this model and so must be addressed through prior processing. The two-term Fatti approximation (Fatti et al. 1994, equation 4) is used to approximate the offset dependent reflectivity over some predefined angle range. The AVO NMO model (Downton and Lines, 2002) solves for the reflectivity over some target window given the source wavelet. By incorporating NMO in the inverse problem, distortions introduced by NMO stretch can be avoided. This linear model written in matrix notation as

$$\mathbf{d} = \mathbf{L}\mathbf{m}, \quad (1)$$

where  $\mathbf{L}$  is the linear AVO NMO operator,  $\mathbf{d}$  is the data vector in equation and,  $\mathbf{m}$  is the unknown parameter vector describing the reflectivity. The data vector contains  $N$  time samples by  $M$  offsets while the parameter vector contains  $2M$  elements. This paper assumes the likelihood function is Gaussian for simplicity but it might be more appropriate for real seismic data to choose a robust distribution.

### **Prior model**

Rather than solving for the P- and S-impedance reflectivity, we choose to solve for the P-impedance and fluid stack reflectivity since these two variables are uncorrelated. If we make the typical assumption made in deconvolution that the reflectivity from different interfaces is uncorrelated, the resulting parameter covariance matrix is diagonal. The fluid stack reflectivity is sparse by its nature since it only responds to anomalous fluids. The P-impedance reflectivity may also be modeled as a long tailed distribution (Levy and Fullagar, 1991). Thus the two reflectivity series can be modeled by a variety of distributions including the Huber, Cauchy or  $L_p$  norm. Good results were obtained with each of these, but for illustration purposes this paper uses the  $L_p$  prior. Sacchi (1999) shows that for the case when  $p=1$  this leads to a prior of the form

$$\frac{\partial J_q}{\partial m_j} = \mathbf{Q}\mathbf{m}, \quad (2)$$

where  $J$  is the objective function and  $\mathbf{Q}$  is a diagonal matrix that is defined as

$$Q_{kk} = \frac{1}{\sigma_m^2} \begin{cases} \frac{1}{\varepsilon} & \left| \frac{m_k}{\sigma_m} \right| < \varepsilon \\ \frac{1}{\left| \frac{m_k}{\sigma_m} \right|} & \left| \frac{m_k}{\sigma_m} \right| \geq \varepsilon \end{cases} \quad (3)$$

where  $\sigma_m$  is the L1 standard deviation of the reflectivity and  $\varepsilon$  is some user chosen threshold. This covariance matrix must be calculated iteratively in a bootstrap fashion outlined below.

### Nonlinear inversion

The Likelihood function (*Equation 1*) may be combined with the *a priori* probability function (*Equation 2*) using Bayes' theorem. There is no explicit interest in the variance of the time-domain constraints so it is marginalized (Sivia, 1996). The most likely solution can then be found by finding where the PDF is stationary. This involves taking the partial derivatives with respect to each parameter, setting the result to zero, and solving the set of simultaneous equations. This results in the nonlinear equation

$$[\mathbf{L}^T \mathbf{L} + \mu \mathbf{Q}] \mathbf{m} = \mathbf{L}^T \mathbf{d}, \quad (4)$$

where  $\mu = \varepsilon^T \varepsilon / (MN - 1)$  and  $\varepsilon = \mathbf{Lm} - \mathbf{d}$ . There are two sources of nonlinearity in *Equation (4)*, the estimate of the regularization parameter  $\mu$  and the calculation of  $\mathbf{Q}$ .

The actual inverse problem being quite large is most efficiently solved using iterative techniques such as conjugate gradient (Skewchuk, 1994). Solving the inverse problem requires two nested loops. In the inner loop the conjugate gradient algorithm is used to solve *Equation 4* using the previously calculated values of  $\mu$  and  $\mathbf{Q}$ . The maximum number of conjugate gradient iterations is used as a parameter to help stabilize the solution (Hansen, 1998). After solving for the reflectivity the estimate of  $\mu$  and the covariance matrix  $\mathbf{Q}$  is updated. Iteratively updating these parameters and re-estimating the reflectivity parameters constitute the outer loop. Generally a satisfactory sparse solution is obtained after 3 to 5 outer loops. For the first loop the inversion is run as an unconstrained inversion by setting  $\mu=0$ . Care must be taken in the first outer loop not to put too much detail in the solution or the problem will not converge. This can be controlled by carefully setting the maximum number of conjugate gradient iterations parameter to a value that limits resolution.

## Example

*Fig. 1* shows the density, P- and S-velocity model used to generate the synthetic gather used in the testing. The S-velocity for most of the model follows the mudrock line. There are 3 anomalous zones off the mudrock line simulating gas zones, a 3 m gas zone at 1.16s, a 23 m gas zone at 1.234 s, and a 13 m gas zone at 1.332 s. The synthetic gather (*Fig. 2*) was generated using raytracing and the reflectivity is generated by the Zoeppritz equation. The model was convolved with a 5/10-60/70 Hz zero-phase wavelet and noise was added to attain a 4:1 signal-to-noise ratio.

*Fig. 3* shows the result of a traditional AVO analysis performed on NMO corrected gathers. Note the high level of noise on the S-impedance reflectivity. The fact that the S-impedance reflectivity is so noisy is a consequence of the random and theoretical noise introduced by the NMO stretch being amplified by the inversion process. The fluid reflectivity has less uncertainty in comparison with the S-impedance reflectivity (Downton and Lines, 2001) and shows all 3 anomalies. However, there is still poor separation of the anomalies from the background noise particularly for the 3 m gas sand.

*Fig. 4* shows the filtered response of the new methodology. For comparison sake it is shown with the same filter as the result in *Fig. 3*. Note the better S/N ratio for both the S-impedance reflectivity and the fluid stack. This is a result of several factors. Firstly, the sparseness constraint reduces the condition number of the Hessian in *equation (4)*. Since the inverse of the Hessian is the parameter uncertainty covariance matrix the resulting estimates are more reliable. Secondly, small eigenvalues are excluded by limiting the number of internal iterations in each conjugate gradient loop, again decreasing the condition number of the Hessian and increasing the stability of the estimate.

*Fig. 5* shows the unfiltered reflectivity estimates. Note the excellent correspondence between the zero offset reflectivity (red) and estimated reflectivity (blue). All three anomalous zones show up on the fluid stack including the 3 m gas sand. The estimated reflectivity is sparse and full spectrum. This result was achieved after 5 external iterations.

## Conclusions

The method shown is an extension of poststack sparse spike deconvolution such as presented in Sacchi (1999) or Trad (2002). Comparing this implementation to the poststack implementation, this method has the advantage that the regularization parameter in *Equation (4)* can be estimated as part of the inversion since the variance of the noise can be estimated from the prestack data. This is not the case for the poststack implementation thus simplifying the implementation. Further by working with prestack data, estimates for both the P-

and S-impedance reflectivity are possible whereas the poststack case only estimates the P-impedance reflectivity.

The results of this approach are superior to that of the traditional approach of first applying NMO and then doing an AVO analysis. In the synthetic example, the new approach was able to more clearly resolve a 3 m gas sand in a layer with a 4000 m/sec velocity and a high cut frequency of 60/70 Hz. Further, the reflectivity estimates of the new method are more reliable than the traditional approach. This is due to the classic trade-off between resolution and reliability. In this case, the improvement in reliability comes at the loss of apparent vertical resolution. Only a sparse reflectivity series is estimated rather than an estimate at every time sample as done by the traditional approach.

### **Acknowledgements**

The authors would like to thank Core Lab, N.S.E.R.C. and the C.R.E.W.E.S. sponsors for funding this research.

### **References**

- Downton, J. E. and Lines, L. R., 2002, AVO NMO, 72 Ann. Internat. Mtg., Soc. Expl. Geophys., Expanded Abstracts
- Downton, J. E. and Lines, L. R., 2001, AVO feasibility and reliability analysis, CSEG recorder, Vol. 26, No 6, pp 66-73
- Fatti, J.L., Smith, G.C., Vail, P.J., Strauss, P.J., and Levitt, P.R., 1994, Detection of gas in sandstone reservoirs using AVO analysis: A 3-D seismic case history using the Geostack technique: *Geophysics*, 59, 1362-1376.
- Hansen, P. H., 1998, Rank-deficient and discrete ill-posed problems: SIAM
- Levy, S. and Fullagar, P. K., 1981, Reconstruction of a sparse spike train from a portion of its spectrum and application to high-resolution deconvolution: *Geophysics*, 46, 1235-1243.
- Sacchi, M. D. and Ulrych, T.D., 1995, High-resolution velocity gathers and offset space reconstruction: *Geophysics*, 60, 1169-1177.
- Sacchi, M. D., 1999, Statistical and transform methods for seismic signal processing, Department of Physics, University of Alberta, available at <http://cm-gw.phys.ualberta.ca/~sacchi/saig/publ.html>
- Sivia, D.S., 1996, Data Analysis, A Bayesian tutorial: Oxford University Press
- Shewchuck, J., 1994, An Introduction to the Conjugate Gradient Method Without the Agonizing Pain, School of Computer Science. Carnegie Mellon University. Pittsburg. available at <http://www-2.cs.cmu.edu/~jrs/jrspapers.html>
- Trad, D., 2002, Implementations and applications of the sparse Radon transform: Ph.D. thesis, University of British Columbia

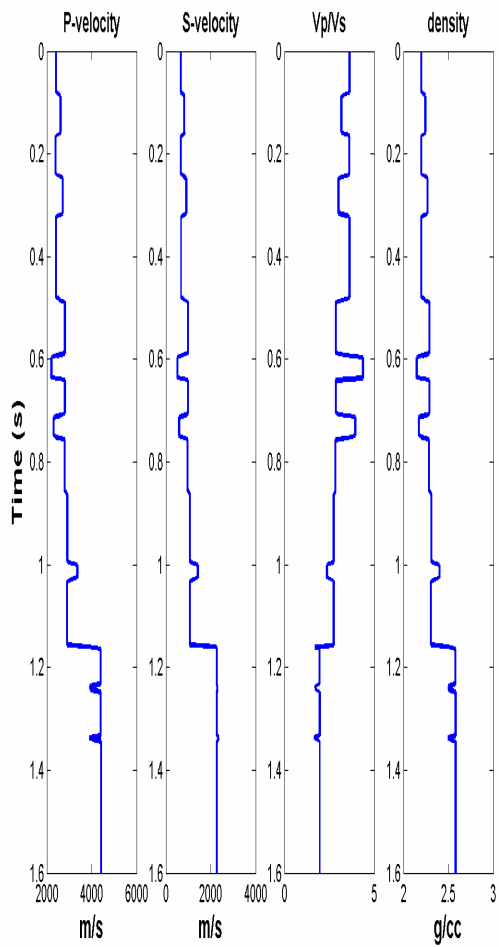


*Fig. 1: Velocity and density input to synthetic model.*

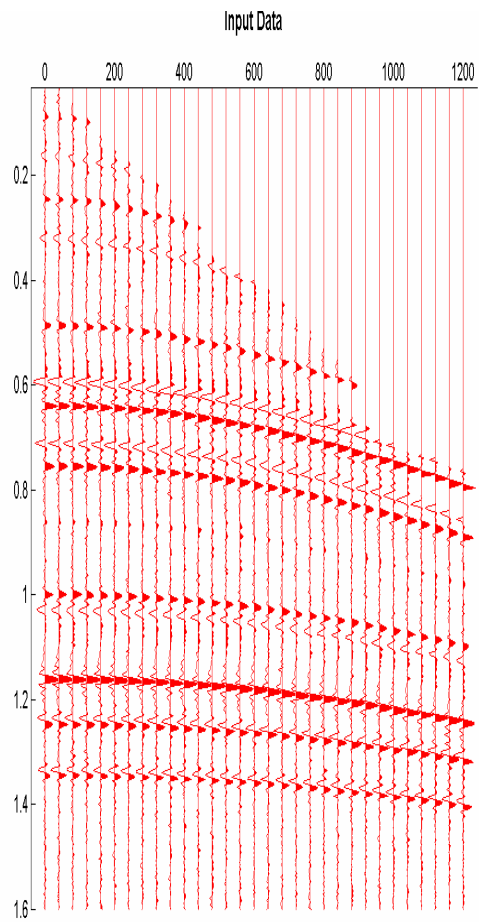


*Fig. 2: Muted synthetic gather generated from input model in fig. 1 with a signal-to-noise ratio of 4.*

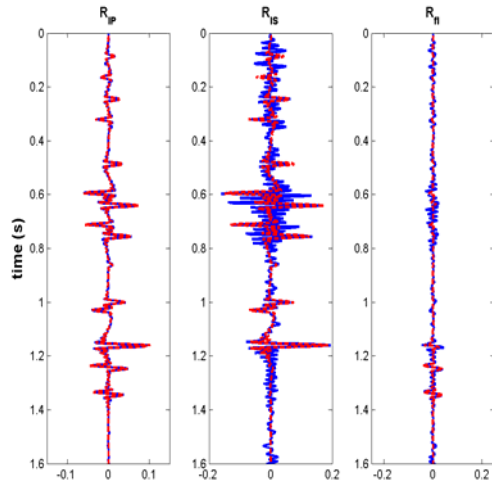


*Fig. 3: AVO inversion results based on traditional methodology of performing AVO on NMO corrected gathers. Actual reflectivity is shown in red and estimate in blue. The first column is P-impedance reflectivity, the second S-impedance reflectivity and the last the fluid stack*

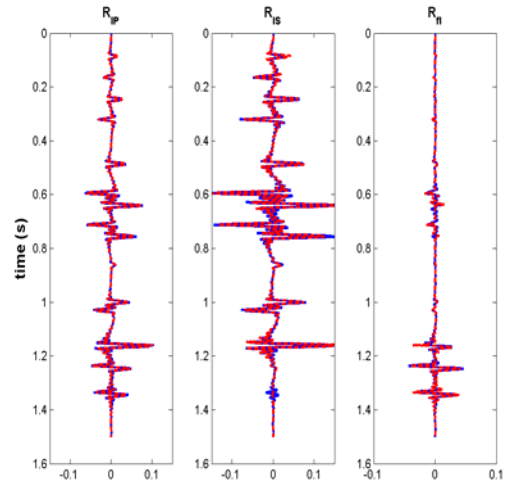


*Fig. 4: Filtered AVO inversion results based on new methodology. Actual reflectivity is shown in red and estimate in blue. The first column is P-impedance reflectivity, the second S-impedance reflectivity and the last the fluid stack.*

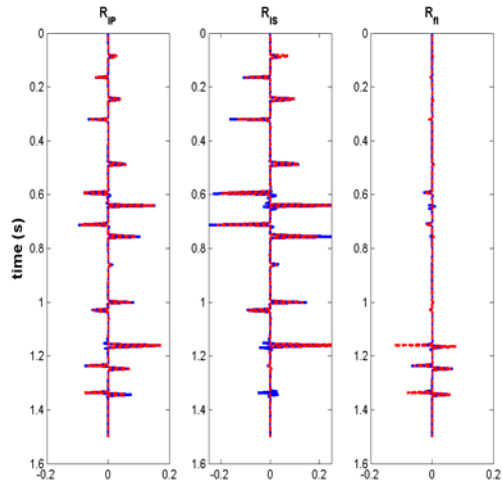


*Fig. 5: Full spectrum AVO inversion results based on new methodology. Actual reflectivity is shown in red and estimate in blue. The first column is P-impedance reflectivity, the second S-impedance reflectivity and the last the fluid stack.*